

ESR and Optical Study of Photo-Orientation in Azobenzene-Containing Liquid-Crystalline Polymer

Alexey V. Bogdanov* and Andrey Kh. Vorobiev

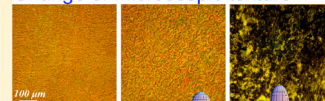
Department of Chemistry, Moscow State University, 119991, Moscow, Russia

S Supporting Information

ABSTRACT: We report a comprehensive experimental study of photoinduced processes in azobenzene-containing liquid-crystalline polymer. The kinetic and optical characteristics of the photoisomerization reaction and photo-orientation process have been determined. The spin probe technique has been used to elucidate the details of orientation order and rotational mobility of molecular fragments within the liquid-crystalline polymer. The evolution of orientation order parameters $\langle P_2 \rangle$, $\langle P_4 \rangle$, and $\langle P_6 \rangle$ in the course of photoinduced ordering of the material as well as the change of liquid-crystalline domain sizes have been studied quantitatively. The obtained experimental results are compared with the predictions of the existing models of photo-orientation.

Azobenzene-containing LC polymer during light irradiation

Change of microscopic texture



Evolution of molecular orientation distribution

INTRODUCTION

The phenomenon of photo-orientation in azobenzene containing media is promising for developing smart photoresponsive materials and data storage devices.^{1–6} Despite numerous potential and already implemented applications, a detailed understanding of the microscopic mechanism of photo-orientation at the present time is lacking. Several physical models, which differ in basic assumptions about the physical origin of photoinduced molecular alignment, were developed for description of this phenomenon.^{7–15} It was posited that photo-orientation is caused by random reorientation of azobenzene fragments during photoisomerization,^{7–10,12} photo-induced rotational diffusion of excited molecules,^{11,12} or reorientation of liquid crystal director due to the torque exerted by a non-equilibrium ensemble of excited chromophores.^{13–15} The detailed experimental information about photochemical properties of the material, characteristics of molecular motions, and parameters of molecular orientation alignment during photo-orientation are necessary for well founded verification of the existing physical models.

In the present work, photo-orientation of azobenzene-containing liquid-crystalline polymer is studied experimentally. Along with the commonly used absorbance spectroscopy with polarized light, the spin probe technique is applied for elucidating the details of molecular orientation in this work. This technique has proven informative for determination of orientation order in liquid-crystalline materials and polymers.^{16,17} It has been shown^{18,19} that orientation order parameters of rank two obtained with this method are consistent with the parameters obtained with optical techniques, but the spin probe technique provides much more detailed information on orientation alignment, including order parameters of higher ranks. In addition to the above-mentioned techniques, we used polarized optical microscopy for monitoring changes in domain structure (texture) of liquid-crystalline material in the course of photoinduced alignment.

The structure of the paper is as follows. Section A contains the experimental details. Section B describes ESR spectra simulation. Section C presents the experimental results. In Section D, experimental data are compared with predictions of existing models of photo-orientation. Section E contains concluding remarks.

A. EXPERIMENTAL DETAILS

Liquid-crystalline copolymer PAAzo6²⁰ (Figure 1a) was chosen in the present work as a test object. This polymer exhibits high efficiency of photo-orientation, low tendency toward chromophore aggregation, and wide temperature range of the nematic phase. Transition temperatures for this material are 24 °C (glass to nematic) and 120 °C (nematic to isotropic).²⁰

A stable nitroxyl radical containing phenyl benzoate moiety²¹ was used as a spin probe (Figure 1b). The anisometric shape of the probe molecule allows it to embed into the liquid-crystalline medium and to efficiently reflect its molecular ordering.²²

The procedure of the sample preparation was the following. The polymer melt was pressed between two glass plates at 120 °C and then cooled to ambient temperature with a rate of ca. 5 °C/min. The film thickness was fixed by glass or PTFE spacers (20–30 μm thick) placed between the glass plates. Before each experiment, the samples were annealed at 60 °C for 2 h to provide the identical thermal history. To obtain aligned samples of PAAzo6, the melted polymer was pressed between glass plates coated with rubbed polyimide and cooled from the isotropic phase to ambient temperature with a rate of 1 °C/min.

To prepare the material for ESR study, chloroform solution with the known content of the polymer was mixed with

Received: August 12, 2013

Revised: September 9, 2013

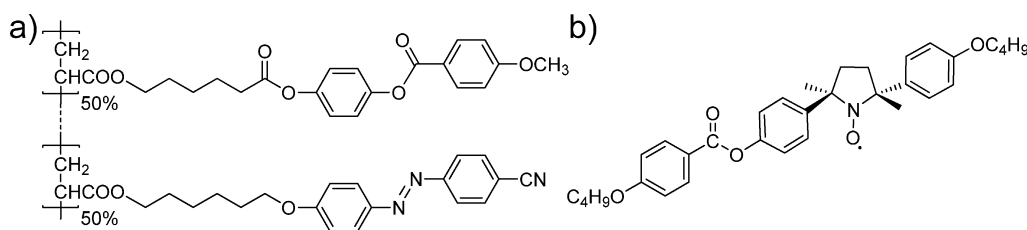


Figure 1. Chemical structure of copolymer PAAzo6 (a) and the spin probe C4 (b), used in the present work.

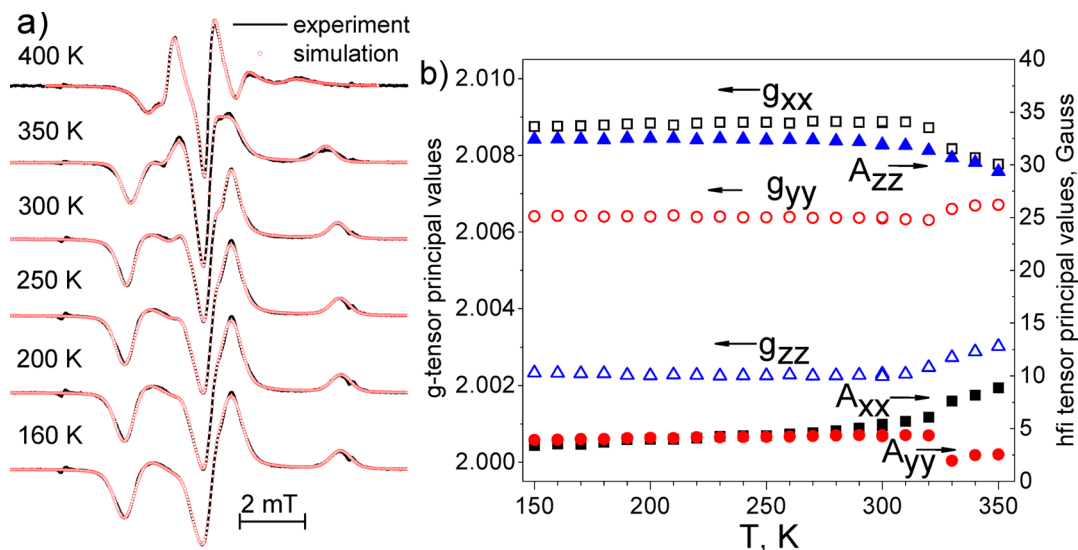


Figure 2. (a) ESR spectra of the spin probe in isotropic samples of PAAzo6 at temperatures of 160–400 K (lines, experiment; circles, numerical simulation result). (b) Temperature dependence of effective spin-Hamiltonian parameters determined from ESR spectra.

chloroform solution of the spin probe. The solvent was evaporated and the mixture was evacuated for a week at 10^{-3} Torr to remove residual chloroform. The concentration of the spin probe in the prepared mixture was 0.5% by weight. Film samples were prepared as described above.

Absorbance spectra were recorded using a Specord M40 UV–vis spectrometer. To account for extinction due to light scattering, the long-wavelength regions of spectra were approximated by a line and these linear baselines were subtracted from the spectra. ESR spectra were recorded with an X-band ESR spectrometer Varian E-3. The magnetic field sweep was calibrated on the third and fourth components of the ESR spectrum of $\text{Mn}^{2+}/\text{MgO}$.

The samples were irradiated with light of high-pressure mercury lamp DRSh-1000, equipped with a water IR filter, a collimating lens system, and a glass filter for isolation of the spectral line with a wavelength of 546 nm. The intensity of the irradiating light was $43\text{ mW}\cdot\text{cm}^{-2}$ (1.2×10^{17} photons $\cdot\text{cm}^{-2}\cdot\text{s}^{-1}$), as measured with a photodiode Vishay-BPW21R. The heating of the sample at this irradiation power was ca. 5–10 °C. This estimate was obtained experimentally using a dummy sample containing a thermocouple. The samples were mounted normally to the irradiating beam propagation direction. The values of absorbance at 546 nm for the studied samples were in the range 0.1–0.6 O.D. At low absorbances in this range, the influence of inhomogeneity of light intensity throughout the film thickness can be neglected. In the case of higher absorbance in this range, the auxiliary time variable $\tilde{t} = \int_0^t (1 - 10^{-D(\tau)}) / (D(\tau) \ln 10) d\tau$ was introduced during

the kinetic analysis to account for nonlinear absorption of light.²³

Optical dichroism of homeotropically aligned samples was measured with the spectrophotometer by the following procedure. Consider the probe beam impinging on the sample at angle β and polarized in the plane of incidence (p-polarization). Let d be the sample thickness. Because of refraction, light propagates within the polymer at angle α to the sample normal ($n \sin \alpha = \sin \beta$, where n is the refractive index). Let $A(\alpha)$ be the experimentally measured value of absorbance for the described probe beam. $A(0)$ is the value of absorbance at normal incidence of the probe beam. The optical path of the beam within the sample is $d/\cos \alpha$. Let A_z denote the absorbance per optical path d for light polarized along the sample normal and propagating along the sample surface. The value $A(\alpha) \cos \alpha$ is the absorbance per optical path d at oblique incidence. This value can be decomposed into two orthogonally polarized components as follows:

$$A(\alpha) \cos \alpha = A_z \sin^2 \alpha + A(0) \cos^2 \alpha \quad (1)$$

Thus, two values of absorbance, measured at normal and oblique incidence of the probe beam, are necessary to calculate the value of sample dichroism. The corresponding expression is the following:

$$\begin{aligned} d &= \frac{A_z - A(0)}{A_z + 2A(0)} \\ &= \frac{A(\alpha) \cos \alpha - A(0)}{A(\alpha) \cos \alpha + A(0)(2 \sin^2 \alpha - \cos^2 \alpha)} \end{aligned} \quad (2)$$

The value of refractive index was taken to be 1.6 on the basis of measurements for similar compounds.²⁴

Microscopic images were obtained with polarizing optical microscopes MIN-8 and Axioscope 40Pol (Carl Zeiss) equipped with CCD cameras. The average size of liquid crystal domains was estimated in the following way. A microscopic image was converted into grayscale and normalized on maximum and minimum intensity. After that, the image was thresholded at half intensity and the number of connected areas n in the resulting binary image was calculated. Domain diameter was estimated as if the domains had effective spherical shape, as $((4/\pi) \cdot (A/n))^{1/2}$, where A is the sample area depicted in the analyzed image.

B. ESR SPECTRA SIMULATION

Numerical simulation of ESR spectra was performed by minimization of the sum of squared deviations of calculated spectra from the experimental ones. The procedure of spectra simulation in the absence of spin probe rotation (rigid limit) is described elsewhere.¹⁶ The orientation distribution function was determined from ESR spectra by a two-step procedure. First, the ESR spectrum of an isotropic sample was simulated. Magnetic parameters of the spin probe in the studied matrix were determined as a result of this simulation. The obtained values of magnetic parameters were used then to simulate angular dependence of the ESR spectrum of the anisotropic sample in the second step. For this, ca. 10 ESR spectra recorded at different orientations of the sample relative to the magnetic field of the ESR spectrometer were simulated jointly. As a result, the orientation characteristics of the probe were determined. Each step is described in more detail below.

ESR spectra of the spin probe in an isotropic sample of PAAzo6 at temperatures of 160–400 K are presented in Figure 2a. The ESR spectra typical for nitroxide spin probes in the absence of molecular rotations were observed at temperatures below 350 K. Numerical simulation of spectra in this temperature range yields the spin-Hamiltonian parameters for the spin probe, i.e., the principal values of the g -tensor and tensor of hyper-fine interaction (hfi) of the unpaired electron with ^{14}N nucleus.¹⁶ The temperature dependence of spin-Hamiltonian parameters is presented in Figure 2b, and the values of parameters at 295 K are listed in Table 1. In Figure

Table 1. Spin-Hamiltonian Parameters, Determined from the ESR Spectrum of an Isotropic Sample of PAAzo6 at 295 K

	g		hfi (10^{-4} T)
g_{xx}	2.008878	A_{xx}	5.25
g_{yy}	2.006374	A_{yy}	4.28
g_{zz}	2.002248	A_{zz}	32.15

2b, it is seen that below 300 K magnetic parameters are nearly temperature independent. The principal values of g - and hfi-tensors at higher temperatures (300–350 K) become partially averaged by the probe rotational movements. ESR spectra in these conditions can be simulated in the framework of the quasi-libration model,²⁵ which takes account of amplitude restricted high-frequency angular vibrations of the probe molecules.

At higher temperatures (350–393 K), the process of the polymer alignment by the magnetic field of the ESR spectrometer was observed. This process in the magnetic

field 0.33 T takes ca. 3000, 1000, and 300 s at temperatures of 350, 380, and 390 K, correspondingly. The orientation induced by magnetic field complicates the recording of isotropic ESR spectra in this temperature range but can be used for estimation of molecular mobility in the medium. A model of field-induced alignment has been suggested by Osipov and Terentjev.²⁶ This model provides an expression relating the time of macroscopic orientation of liquid crystal with the characteristic time of molecular rotations. In accordance with this model,²⁶ rotation correlation times of mesogenic molecular fragments in the studied material can be estimated using the following expression:

$$\tau_{R,\perp} = \frac{\Delta\chi B^2}{\mu_0 N_A k_B T} \cdot \frac{1}{\sqrt{T_c \langle P_2 \rangle / T} e^{T_c \langle P_2 \rangle / T}} \tau_H \quad (3)$$

where τ_H is the characteristic time of liquid crystal orientation in the magnetic field with flux density B , $\tau_{R,\perp}$ is the rotation correlation time of mesogenic molecular fragments of the liquid crystal, $\Delta\chi$ is the anisotropy of magnetic susceptibility, T_c is the temperature of nematic to isotropic transition, and $\langle P_2 \rangle$ is the order parameter of the aligned material.

With the values $\Delta\chi \sim 5 \times 10^{-5} \text{ cm}^3 \cdot \text{mol}^{-1}$,²⁷ $B = 0.33 \text{ T}$, $T_c = 393 \text{ K}$, and $\langle P_2 \rangle \approx 0.7$, an estimate for rotation correlation times of mesogenic fragments is $\tau_{R,\perp} \sim 3 \times 10^{-7}$ to $3 \times 10^{-6} \text{ s}$ at 350–390 K. No detectable alignment of PAAzo6 takes place within a period of 1 month at 298 K in the magnetic field 1 T. Using eq 3, one can obtain a lower estimate for rotation correlation time at 298 K, $\tau_{R,\perp} > 10^{-2} \text{ s}$.

The ESR spectra of the spin probe in the isotropic phase of PAAzo6 ($T > 393 \text{ K}$) were successfully simulated with the model of anisotropic Brownian diffusion (Figure 2a, 400 K). These simulations were performed using the program described by Budil et al.²⁸ The values of rotation correlation times at 400 K were found to be $\tau_{\parallel} = 5.1 \times 10^{-10} \text{ s}$ and $\tau_{\perp} = 7.3 \times 10^{-8} \text{ s}$.

Characteristics of molecular orientation in aligned samples of PAAzo6 were determined from ESR spectra angular dependencies recorded at 295 K. At this temperature, the alignment of the studied polymer is not affected by the spectrometer magnetic field, and ESR spectra are not complicated with molecular rotation effects.

Orientation alignment was characterized by the orientation distribution function defined as the probability density to find spin-probe particles directed at a certain angle:

$$\rho(\Omega) = \frac{dN(\Omega)}{d\Omega} \quad (4)$$

where $\Omega = (\alpha, \beta, \gamma)$ are Euler angles relating the reference frame of the sample with the molecular reference frame, $d\Omega = d\alpha \sin\beta d\beta d\gamma$. The orientation distribution function was represented as an expansion in a series of Wigner D-functions, truncated at the maximum rank J_{\max} :

$$\rho(\Omega) \approx \sum_{j=0}^{J_{\max}} \sum_{m=-j}^j \sum_{n=-j}^j \frac{2j+1}{8\pi^2} A_{mn}^j D_{mn}^j(\Omega) \quad (5)$$

where A_{mn}^j is a set of order parameters, defined as

$$A_{mn}^j = \int \mathcal{D}_{mn}^{j*}(\Omega) \rho(\Omega) d\Omega \quad (6)$$

The order parameter A_{00}^0 is equal to unity, since the distribution function is normalized.

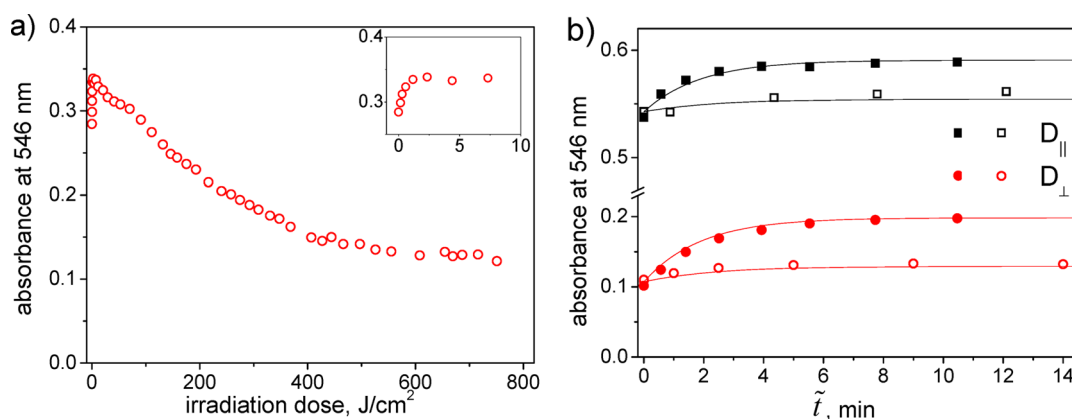


Figure 3. (a) Kinetics of absorbance change upon irradiation of PAAzo6 with non-polarized light ($\lambda = 546$ nm). (b) Kinetics of polarized absorbance change upon polarized irradiation of 546 nm of the PAAzo6 sample aligned with the rubbed surface; spectrophotometer probe beam polarized parallel (squares) and perpendicular (circles) with respect to the sample director; irradiating light polarized parallel (filled symbols) and perpendicular (open symbols) with respect to the sample director; time variable $\tilde{t} = \int_0^t (1 - 10^{-D(\tau)}) / (D(\tau) \ln 10) d\tau$ is introduced to account for nonlinear light absorption.

Orientation order parameters of the spin probe characterize the alignment of the matrix most reliably if the molecular reference frame is associated with the Saupe ordering tensor.²⁹ The shape of the ESR spectrum depends on the relative orientation of principal axes of the \mathbf{g} -tensor and the ordering tensor in the spin probe molecule,^{16–19,22} and therefore, the analysis of ESR spectra provides a possibility to determine the direction of orientation axes in the probe molecule.

The symmetry of the experimental system imposes certain constraints on the possible values of order parameters A_{lm}^i .^{30,31} It should be noted that, if the orientation distribution function is not dependent on Euler angles α and γ (the case of axial probe molecules distributed in an axial sample), the only nonzero order parameters are A_{0j}^i with even j . In this case, the alignment of the sample is commonly characterized with order parameters $\langle P_j \rangle = A_{0j}^i$.

The least-squares simulation of ESR spectrum angular dependence of aligned sample yields the following: (i) the truncation value J_{\max} selected so that the increase of J_{\max} does not lead to further improvement in the description of spectra; (ii) the set of orientation order parameters A_{lm}^i for the chosen symmetry; (iii) the direction of ordering tensor axes in the reference frame of the \mathbf{g} -tensor.

C. EXPERIMENTAL RESULTS

C.1. Photoisomerization of PAAzo6. The UV–vis spectrum of copolymer PAAzo6 in solution is typical for absorbance spectra of *trans*-azobenzene derivatives. A π – π^* band with the maximum at 365 nm and an n – π^* band at 430–600 nm are observed. Upon irradiation of PAAzo6 in solution with UV light, absorption increases in the n – π^* band and decreases in the π – π^* band. It is well established in the literature³² that these changes are caused by *trans*-to-*cis* photochemical isomerization of azobenzene units. Irradiation induces both *trans*-to-*cis* and *cis*-to-*trans* photoisomerization because of the overlap of *trans* and *cis* isomer absorption bands. In addition, thermal *cis*-to-*trans* isomerization takes place. Thus, irradiation of a solution leads to a photostationary state, in which the *trans*-to-*cis* photoisomerization rate is equal to the sum of photochemical and thermal *cis*-to-*trans* isomerization rates. This photostationary state almost in all cases contains

certain amounts of the photochrome in *cis* and *trans* configurations.

The films of PAAzo6 with thickness 20–30 μm were used in the present work. Only the long-wavelength edge of the n – π^* band can be observed in this case due to large absorption. Figure 3a shows the kinetics of absorbance change upon the irradiation of PAAzo6 sample with non-polarized light of 546 nm wavelength. The increase of absorbance in the n – π^* band is observed at small irradiation doses. This increase is associated with the establishment of a photostationary state of photoisomerization (Figure 3a, inset). The photostationary state was achieved with an effective rate constant of 0.10 s^{-1} (irradiation intensity 43 $\text{mW}\cdot\text{cm}^{-2}$). The rate constant of thermal *cis*-to-*trans* isomerization was measured in a separate experiment and was found to be $(5.1 \pm 0.1) \times 10^{-3} \text{ min}^{-1}$ at 298 K. Thus, thermal isomerization is characterized by a negligibly small rate in comparison with photochemical reactions.

Photoisomerization kinetics in anisotropic azobenzene-containing sample provides information about optical and photochemical properties of azobenzene moieties in the material. Absorbance coefficients of *trans*- and *cis*-azobenzene units depend on the relative orientation of the electric field vector of light and the axis of the sample anisotropy. As shown in Appendix A of the Supporting Information, the value of the absorbance coefficient for linearly polarized light is given by the expression

$$\varepsilon_i(\Theta) = \bar{\varepsilon}_i [1 + 2d_i p_i P_2(\cos \Theta)] \quad (7)$$

Here index i denotes the *trans* or *cis* isomer, Θ is the angle between the electric field vector of light and the sample director, $\bar{\varepsilon}_i$ is the average extinction coefficient, d_i is the molecular linear dichroism, $p_i = \langle A_{0,0}^2 \rangle_i$ is the orientation order parameter of rank two for isomer i , and $P_2(\cos \Theta) \equiv (3 \cos^2 \Theta - 1)/2$. Expression 7 is derived in the assumption of the axially symmetric extinction coefficient tensor of the chromophore.

As shown in Appendix B of the Supporting Information, the growth of the *cis*-azobenzene molar fraction $x_c(t)$ is described by the following expression:

$$x_c(t) = (1 - \exp[-I \ln 10 \{ \varepsilon_c \varphi_{tc} + \varepsilon_c \varphi_{ct} \} \tilde{t}]) \cdot \frac{\varepsilon_t \varphi_{tc}}{\varepsilon_t \varphi_{tc} + \varepsilon_c \varphi_{ct}} \quad (8)$$

where I is the intensity of irradiating light (in $\text{Einstein}\cdot\text{s}^{-1}\cdot\text{cm}^{-2}$), φ_{tc} and φ_{ct} are quantum yields of trans-to-cis and cis-to-trans photoisomerization, and ε_{t} and ε_{c} are absorption coefficients of *trans*- and *cis*-azobenzene units. The absorption coefficients ε_{t} and ε_{c} in expression 8 are averaged over the orientation distribution of chromophores and taken for wavelength and polarization of irradiating light. The values of these coefficients are given by eq 7. The variable $\tilde{\tau} = \int_0^t (1 - 10^{-D(\tau)}) / (D(\tau) \ln 10) d\tau$ is introduced to account for nonlinear absorption of light in optically dense sample.²³

The kinetics of the cis fraction change $x_{\text{c}}(t)$ given by eq 8 defines the observed kinetics of absorbance change:

$$D(t) = lc_0\{(1 - x_{\text{c}}(t))\varepsilon_{\text{t}} + x_{\text{c}}(t)\varepsilon_{\text{c}}\} \quad (9)$$

where l is the sample thickness, c_0 is the total concentration of azobenzene units, and ε_{t} and ε_{c} here represent absorption coefficients of *trans*- and *cis*-azobenzene units for *probe* light polarization and wavelength, averaged over the orientation distribution of chromophores.

The experimentally observed change of the polarized absorbance in the course of polarized irradiation of PAAzo6 sample aligned with a rubbed polyimide surface is presented in Figure 3b. D_{\parallel} and D_{\perp} in the figure represent optical densities at parallel and perpendicular directions of the electric field vector of the spectrophotometer probe beam with respect to the sample director. Filled circles correspond to irradiation with light polarized along the director, and open circles show irradiation with light polarized perpendicularly to the director. The result of least-squares fitting of experimental data with eqs 8 and 9 is shown in Figure 3b with lines. The values of photochemical and optical characteristics obtained in the course of the fitting are presented in Table 2. The value $r_{\varepsilon} = \bar{\varepsilon}_{\text{c}}/\bar{\varepsilon}_{\text{t}}$ is the ratio of average extinction coefficients for trans and cis isomers, $r_{\phi} = \varphi_{\text{ct}}/\varphi_{\text{tc}}$ is the ratio of quantum yields.

Table 2. Photochemical Characteristics of *trans*- and *cis*-Azobenzene Units in PAAzo6^a

$d_{\text{t}}p_{\text{t}}$	0.576 ± 0.016
$d_{\text{c}}p_{\text{c}}$	0.034 ± 0.017
r_{ε}	3.44 ± 0.10
r_{ϕ}	4.10 ± 0.11
$\bar{\varepsilon}_{\text{t}}lc_0$	0.252 ± 0.003
$I\varphi_{\text{tc}}/lc_0$	$(0.053 \pm 0.001) \text{ min}^{-1}$

^aThe values are obtained by the analysis of photoisomerization kinetic curves. All values correspond to a wavelength of 546 nm.

The average molar mass of the material PAAzo6 is 790 g/mol of azobenzene groups. Assuming the density of the material is equal to ca. $1 \text{ g}\cdot\text{cm}^{-3}$, the concentration of azobenzene units can be estimated as $c_0 \approx 1.3 \text{ mol}\cdot\text{L}^{-1}$. In the described experiment, the irradiating light intensity was $I = 3.14 \text{ mW}\cdot\text{cm}^{-2}$ and the sample thickness was $l = 20 \mu\text{m}$. Using the obtained value $I\varphi_{\text{tc}}/lc_0 = 0.053 \pm 0.001 \text{ min}^{-1}$, one can estimate isomerization quantum yields: $\varphi_{\text{tc}} = 0.16$, $\varphi_{\text{ct}} = \varphi_{\text{tc}}\cdot r_{\phi} = 0.66$. From the measured value $\bar{\varepsilon}_{\text{t}}lc_0 = 0.252$, one can deduce $\bar{\varepsilon}_{\text{t}} = 100 \text{ L}\cdot\text{mol}^{-1}\cdot\text{cm}^{-1}$ and $\bar{\varepsilon}_{\text{c}} = r_{\varepsilon}\bar{\varepsilon}_{\text{t}} = 344 \text{ L}\cdot\text{mol}^{-1}\cdot\text{cm}^{-1}$ for average extinction coefficients.

In Table 3, optical and photochemical characteristics measured for PAAzo6 are compared with those found in the literature for azobenzene derivatives in solutions, liquid crystals, and polymers. It can be seen that photochemical characteristics for different azobenzene derivatives and different matrixes differ

significantly. Nevertheless, photochemical characteristics measured for PAAzo6 in this work are in general agreement with the literature data.

Values $d_{\text{t}}p_{\text{t}}$ and $d_{\text{c}}p_{\text{c}}$ presented in Table 3 reflect important features of orientation order of *trans*- and *cis*-azobenzene fragments. The $n-\pi^*$ transition in *trans*-azobenzene is known to be characterized by high polarization.^{36,37} Assuming that the characteristic of transition polarization is close to unity ($d_{\text{t}} = 1$), the obtained value of $d_{\text{t}}p_{\text{t}}$ leads to an estimate of order parameter $p_{\text{t}} \sim 0.6$. It means that *trans*-azobenzene moieties are strongly ordered. The product $d_{\text{c}}p_{\text{c}}$ for the *cis*-azobenzene fragment is smaller than that for the *trans*-azobenzene fragment. It may be caused both by poorer alignment of *cis*-azobenzene fragments in liquid-crystalline material¹⁹ and by weaker polarization of the $n-\pi^*$ transition in *cis*-azobenzene due to intramolecular rotation of benzene rings.³⁶

On the basis of the obtained data, one can estimate the molar fraction of the cis isomer in the photostationary state of isomerization at an irradiating wavelength of $\lambda = 546 \text{ nm}$. The photostationary cis fraction for isotropic sample can be calculated using eq 8 as follows:

$$x_{\text{c}} = \frac{\bar{\varepsilon}_{\text{t}}\varphi_{\text{tc}}}{\bar{\varepsilon}_{\text{t}}\varphi_{\text{tc}} + \bar{\varepsilon}_{\text{c}}\varphi_{\text{ct}}} = \frac{1}{1 + r_{\varepsilon}r_{\phi}} = 0.066 \quad (10)$$

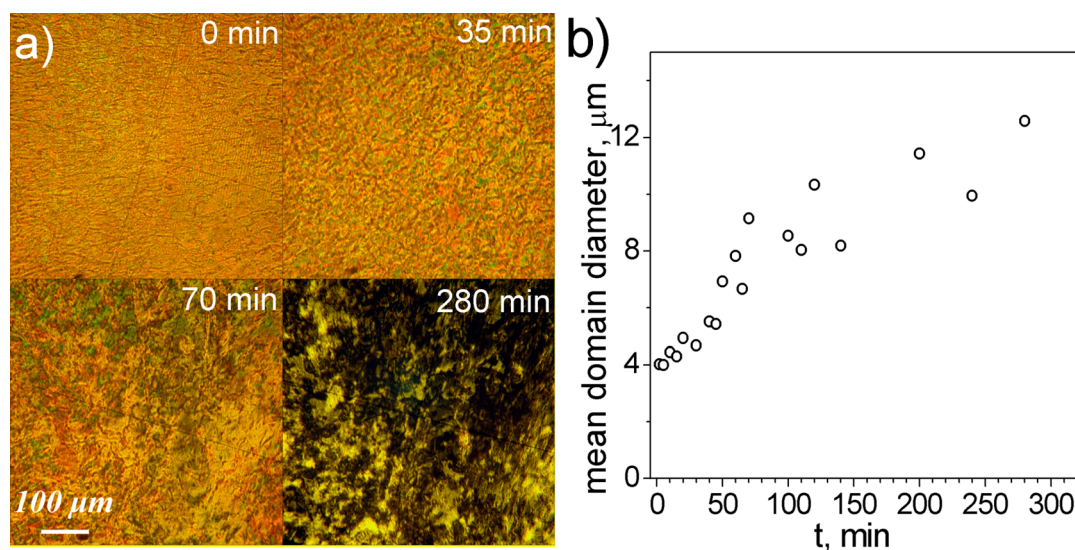
C.2. Photo-Orientation of PAAzo6. Figure 3a shows that absorbance in the $n-\pi^*$ band decreases upon prolonged irradiation of the initially isotropic PAAzo6 sample. This process is associated with photoinduced alignment of azobenzene chromophores perpendicular to the surface of the irradiated sample. The dichroism along the sample normal was determined from absorbance spectra recorded at normal and oblique incidence of the spectrophotometer probe beam, as described in section A (eq 2). The value of photoinduced dichroism after long (1920 min) irradiation was found to be 0.69 ± 0.10 . To exclude the influence of *cis*-azobenzene moieties on the spectra, the sample was left for 16 h in the dark after the illumination and prior to dichroism measurements. This time is sufficient for the completion of thermal cis-to-trans isomerization.

The process of photoinduced alignment is accompanied with the change of microscopic texture of the polymer sample (Figure 4a). Due to photoinduced homeotropic (i.e., in the direction perpendicular to film surface) alignment of the liquid crystal director, the image between crossed polarizers becomes darker. As seen in Figure 4a, the sizes of liquid-crystalline domains notably increase in the course of irradiation. An estimate of mean domain sizes was obtained from calculation of the number of connected areas in thresholded microscopic images, as described in section A. The kinetics of mean domain size change is presented in Figure 4b.

The evolution of orientation distribution function during photo-orientation was measured with the spin-probe technique described in section B. The application of this procedure is illustrated in Figure 5 for a sample of PAAzo6 aligned with magnetic field (0.33 T, 350 K). The experimental angular dependence of the ESR spectrum and the results of simulation are presented in Figure 5a. Figure 5b depicts the molecular model of the central structural unit of the spin probe. This model is built up on the basis of X-ray diffraction data.²¹ Directions of g-tensor principal axes are shown in Figure 5b as black arrows. The long thick arrow represents the direction of the ordering principal axis (the orientation axis), which was

Table 3. Literature Data on Photochemical Characteristics of Azobenzene Derivatives in Solutions, Liquid Crystals, and Polymers

photochromic molecule	matrix	λ (nm)	d_p	d_c	r_e	φ_{lc}	φ_{ct}	ref
azobenzene	hydrocarbon solution	440			3.09	0.20–0.36	0.40–0.75	32
azobenzene	5CB/PPE	436	0.43	0.18				19
S1			0.39	0.19				
S2			0.36	0.14				
DO3	8CB, SmA	488	0.5–0.6	0.1–0.15				33
	8CB, N		0.35–0.5	0.1				
MR	8CB, SmA	488	0.4–0.46	0.1		0.17–0.22	0.37–0.45	
			0.26–0.4	0.1		0.22	0.28	
	8CB, N							
DR1	PMMA	488–547				0.11	0.7	34
PUR-1		488			1.95	0.004	0.57	35
PUR-2					1.95	0.007	0.29	
PUR-3					5.44	0.011	0.21	
PUR-4					5.44	0.017	0.29	
PAAzo6		546	0.576	0.034	3.44	0.16	0.66	this work

**Figure 4.** Microscopic images of the PAAzo6 sample between crossed polarizers, taken at different irradiation times (a) and kinetics of mean domain size change in the course of photo-orientation (b). Sample thickness 25 μm .

determined as the result of numerical simulation of the spectra. It is seen that this direction coincides with the long molecular axis. Thus, as it might be expected, rod-like spin probe molecules in liquid-crystalline medium align with their long axes parallel to the LC director. A similar direction of orientation axis for the same spin probe was determined earlier as a result of the study of its alignment in low molecular weight liquid crystals.³⁸ Figure 5c shows the orientation distribution function of the molecular orientation axis in the reference frame of the sample. Orientation order parameters associated with this distribution function are listed in Table 4 (first column). The value of the order parameter of rank two $\langle P_2 \rangle = 0.602$ in PAAzo6 is in agreement with order parameters commonly measured for nematic matrices.

To determine the evolution of orientation distribution of PAAzo6 during photo-orientation, the polymer sample containing the spin probe was irradiated with non-polarized light of 546 nm over a certain time interval. After this, the angular dependence of the ESR spectrum for the irradiated sample was recorded. The angular dependences were simulated as described in section B. The change of obtained orientation

distribution is illustrated in Figure 6a. The initially isotropic orientation distribution is observed to become anisotropic in the course of irradiation. The director of PAAzo6 aligns perpendicular to the sample surface, i.e., in the direction of irradiating light propagation. Thus, the observed direction of preferential orientation is consistent with literature data that demonstrate that irradiation of azobenzene-containing materials leads to their alignment perpendicular to the electric vector of irradiating light polarization.^{1–6,39,40}

It has been found in separate experiments that ESR spectra recorded immediately after irradiation of PAAzo6 are identical to those recorded after the completion of thermal cis-to-trans isomerization. Obviously, the corresponding orientation distribution functions were found to be identical as well. This observation indicates that the orientation order is the same for PAAzo6 in pure trans form and with the photostationary content (6.6%) of cis isomer.

Irradiation of aligned samples of PAAzo6 leads to photo-induced reorientation. The evolution of the PAAzo6 orientation distribution function during this process is illustrated in Figure 6b. In this experiment, the polymer before

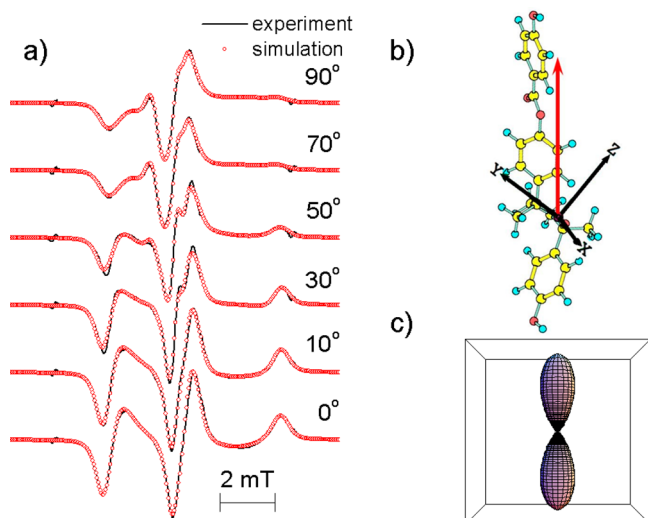


Figure 5. (a) Experimental ESR spectra recorded at different angles (specified near the spectra) between the sample director and the direction of the spectrometer magnetic field (lines) and the results of numerical simulation of these spectra (circles). (b) The molecular model of the spin probe in g-tensor reference frame and the direction of the orientation axis determined in the course of the simulation. (c) The probe orientation distribution function of the orientation axis determined in the course of the simulation.

Table 4. Order Parameters of the Spin Probe in the Polymer PAAzo6 Aligned with Different Orientation Techniques

	alignment technique	
	magnetic field	photo-orientation
$\langle P_2 \rangle$	0.602 ± 0.010	0.78 ± 0.02
$\langle P_4 \rangle$	0.248 ± 0.013	0.506 ± 0.010
$\langle P_6 \rangle$	0.076 ± 0.007	0.214 ± 0.015
$\langle P_8 \rangle$		0.065 ± 0.006

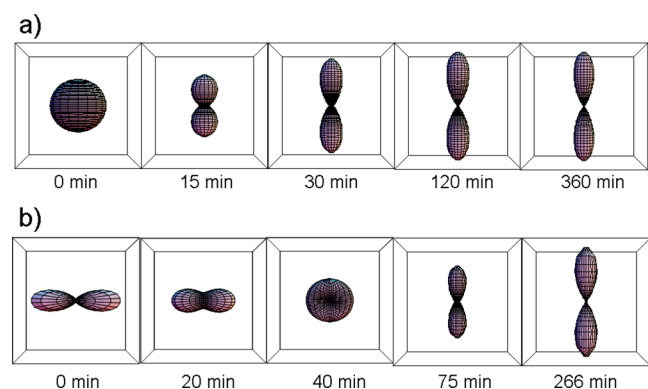


Figure 6. The change of the orientation distribution function in the course of photo-orientation (a) and photo-reorientation (b) in PAAzo6 upon irradiation with non-polarized light ($\lambda = 546$ nm).

irradiation was aligned with the magnetic field (0.5 T) at 360 K along the film surface. The photo-orientation process induced by irradiation is seen as the decrease of orientation distribution anisotropy at first and then the increase of the anisotropy in the new direction. The assumption of axial orientation distribution (along the preferential orientation direction) was sufficient for a satisfactory description of experimental ESR spectra. The only exception were ESR spectra recorded at 40 min of irradiation. These spectra were simulated successfully only with the

account of oblateness of orientation distribution function along the direction perpendicular to both the initial and final orientations of the material.

Anisotropy of orientation distribution can be quantitatively characterized with orientation order parameters (eq 6). The kinetics of the change of order parameters during photo-orientation and photo-reorientation are presented in Figure 7a and b, respectively. Figure 7a (right scale) also illustrates the change of absorbance during irradiation. It is seen that the slow process of absorbance decrease corresponds to photo-orientation.

The values of orientation order parameters for the polymer aligned by a magnetic field (0.33 T, 360 K) and by light irradiation (1920 min) are compared in Table 4. Apparently, the action of light leads to a much higher degree of order. The value of photoinduced dichroism obtained from optical measurements (0.69 ± 0.10) is in agreement with the results obtained with the spin probe technique (0.78 ± 0.02).

Figure 8 illustrates the temperature dependence of photo-orientation rate. The kinetics of the change of the order parameter $\langle P_2 \rangle$ during photo-orientation at temperatures of 5–72 °C is presented in the figure. It was found that in the nematic phase of PAAzo6 ($t > 24$ °C) the initial rate of photo-orientation has a small temperature dependence, and the final value of photoinduced dichroism somewhat decreases with the increase of temperature. In the glassy state ($t < 24$ °C), the rate of photo-orientation is significantly suppressed.

D. DISCUSSION

The obtained experimental results should be considered in the light of existing theoretical models of the photo-orientation process. Most models rest upon the assumption of random reorientations of azobenzene chromophores in the course of cycles of trans–cis–trans photoisomerization. In the simplest case, this model leads to the following kinetic equations for orientation distribution functions of the isomers:^{7–9}

$$\left\{ \begin{aligned} \frac{dn_t(\theta)}{dt} &= -I \ln 10 \varphi_{tc} \varepsilon_t(\theta) n_t(\theta) \\ &\quad + I \ln 10 \varphi_{ct} \int \varepsilon_c(\theta') n_c(\theta') \\ &\quad \quad \times R_{CT}(\theta' \rightarrow \theta) d\theta' \\ \frac{dn_c(\theta)}{dt} &= I \ln 10 \varphi_{ct} \varepsilon_c(\theta) n_c(\theta) \\ &\quad - I \ln 10 \varphi_{tc} \int \varepsilon_t(\theta') n_t(\theta') \\ &\quad \quad \times R_{TC}(\theta' \rightarrow \theta) d\theta' \end{aligned} \right. \quad (11)$$

In eq 11, θ is the angle between the principal axis of extinction coefficient and the symmetry axis of the irradiating light (electric field vector in the case of linearly polarized light or propagation direction in the case of non-polarized light). $n_i(\theta) d\theta$ is the amount of isomer i (trans or cis) with orientations in the range $\theta \dots \theta + d\theta$, I is the light intensity, φ_{ct} and φ_{tc} are quantum yields of cis-to-trans and trans-to-cis isomerization, and $\varepsilon_c(\theta)$ and $\varepsilon_t(\theta)$ are absorption coefficients, which depend on molecular orientation. The functions $R_{TC}(\theta' \rightarrow \theta)$ and $R_{CT}(\theta' \rightarrow \theta)$ characterize the molecular reorientation probabilities during the elementary act of trans-to-cis and cis-to-trans isomerization. The value $R_i(\theta' \rightarrow \theta) d\theta$ represents the

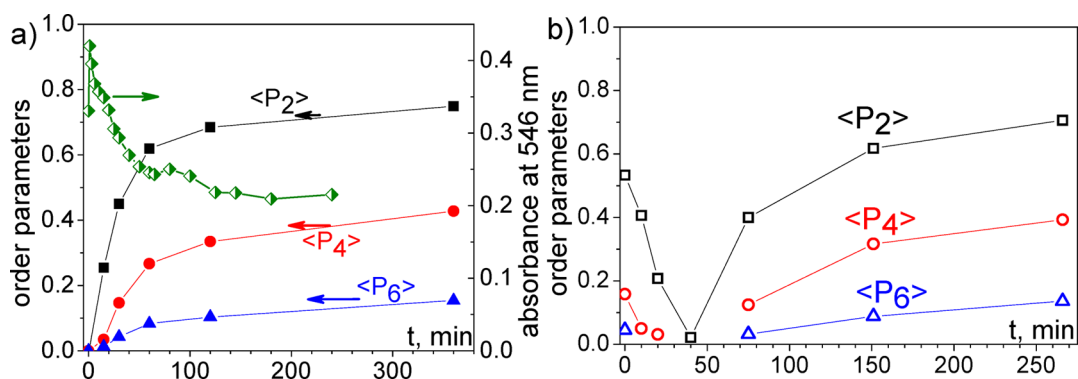


Figure 7. (a) Change of orientation order parameters and absorbance at 546 nm upon irradiation of the initially isotropic PAAzo6 sample with non-polarized light ($\lambda = 546$ nm). (b) Change of order orientation parameters in the course of photo-reorientation.

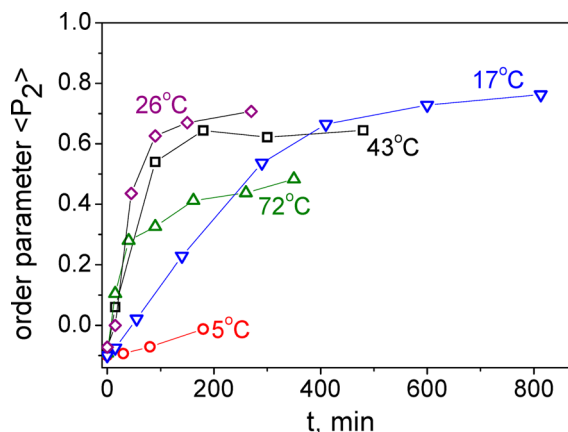


Figure 8. Change of order parameter $\langle P_2 \rangle$ determined with the spin-probe technique during photo-orientation of PAAzo6 at temperatures of 5–72 °C.

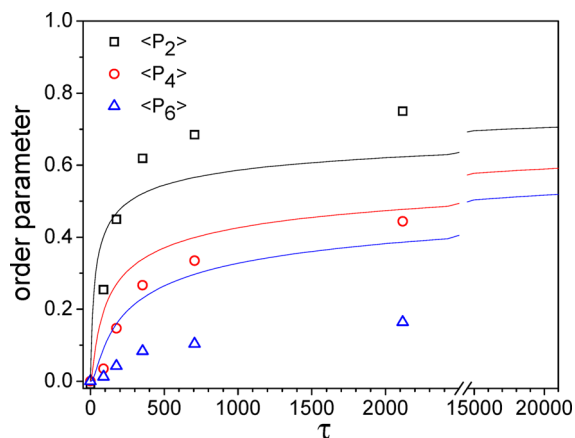


Figure 9. Comparison of orientation order parameters kinetics obtained experimentally (symbols) and predicted by the model of random reorientation during photoisomerization (lines).

probability of the molecule to end up at the angle in the range $\theta \dots \theta + d\theta$, given that it started from the angle in the range $\theta' \dots \theta' + d\theta'$. In the case of random reorientation, probability distributions are isotropic, $R_{TC}(\theta' \rightarrow \theta) = R_{CT}(\theta' \rightarrow \theta) = \sin \theta/2$.

The first term in the right-hand side of the first equation in eq 11 expresses the decrease of the number of *trans*-azobenzene molecules in orientation θ due to photoinduced *trans*-to-*cis* isomerization. The second term expresses the overall rate of increase in the number of *trans* isomers in orientation θ due to *cis*-to-*trans* isomerization from all possible orientations θ' of *cis* isomers. The terms in the second equation in eq 11 have a similar meaning.

The evolution of orientation order parameters in the framework of the random reorientation model can be calculated by integration of eq 11 (Figure 9). In the course of this calculation, the time variable was expressed in units of characteristic times of the establishment of the photostationary state $\tau = t/I \ln 10 (\bar{\epsilon}_i \varphi_{ic} + \bar{\epsilon}_c \varphi_{ci})$ and absorbance coefficients for non-polarized light $\bar{\epsilon}_i(\theta) = \bar{\epsilon}_i [1 - d_i p_i P_2(\cos \theta)]$ ($i = \text{trans, cis}$) were used (see Appendix A in the Supporting Information).

The comparison of the kinetic curves predicted by the random reorientation model with the experimental measurements leads to a conclusion that the model fails to reproduce the kinetics of order parameter growth as well as the ratios between order parameters $\langle P_2 \rangle$, $\langle P_4 \rangle$, and $\langle P_6 \rangle$ which reflect the shape of orientation distribution. The calculated kinetic curves

in Figure 9 are “stretched”; i.e., the rate of photo-orientation substantially decreases when the value of the order parameter $\langle P_2 \rangle \sim 0.5\text{--}0.6$ is achieved. It is seen that in experiment the values of $\langle P_2 \rangle \sim 0.7$ are reached within the time which is an order of magnitude less than predicted by the model.

Modifications of the discussed model that assume reorientations only by a certain angle have been considered.⁴¹ This assumption can be introduced into the model (eq 11) by modifying the reorientation probability densities $R_{TC}(\theta' \rightarrow \theta)$ and $R_{CT}(\theta' \rightarrow \theta)$. Other variations of the model contain additional consideration of orientation distribution for the matrix molecules.^{10,12} This orientation distribution interacts with the orientation distribution of azobenzene fragments through a phenomenological torque. Numerical calculations show that both types of modification, namely, the restriction of turn angle and the account of interaction with the matrix, lead to deceleration of the photo-orientation process. Therefore, they do not provide better correspondence between theoretical predictions and the experimental measurements than that shown in Figure 9.

Another model of photo-orientation is based on the notion of photoinduced rotation diffusion of light absorbing molecules. This idea was initially stated by Albrecht⁴² and later applied to describe photo-orientation of azobenzene-containing materials.^{11,12} The model assumes that dissipation of absorbed photon energy leads to local melting of the matrix in the vicinity of the chromophore and induces the reorientation. Since the

probability to absorb light is different for chromophores with different orientations, this process should lead to the induction of anisotropy of orientation distribution. According to the mathematical model presented by Chigrinov et al.,¹¹ the effective potential which acts on the chromophores due to anisotropy of light absorption is given by the expression

$$\Phi(\theta)kT = \frac{\bar{I}\alpha V_m \tau}{2} \cos^2 \theta \quad (12)$$

and the maximum value of the order parameter $\langle P_2 \rangle$ at linearly polarized irradiation is

$$\langle P_2 \rangle_\infty = -\frac{\bar{I}\alpha V_m \tau}{15kT} \quad (13)$$

In eqs 12 and 13, \bar{I} is the energy flux of the irradiating light, α is the absorbance coefficient, V_m is the molecular volume, kT is the energy of thermal motion, and τ is the time needed for complete dissipation of the energy of absorbed photon. Using the parameters of our experiment ($\bar{I} = 43 \text{ mW}\cdot\text{cm}^{-2}$, $\alpha \sim 100 \text{ cm}^{-1}$, $V_m = 10^{-21} \text{ cm}^3$, $kT \approx 0.4 \times 10^{-20} \text{ J}$, $\tau \sim 10^{-10} \text{ s}$), one can obtain an estimate: $\langle P_2 \rangle_\infty \sim -10^{-12}$ and $\Phi(\theta)kT \sim 10^{-11} kT$. Thus, the considered model predicts a much lower degree of photoinduced order than that observed experimentally. The estimated value of the effective potential is many orders of magnitude smaller than the molecular mean field of liquid-crystalline medium $W_{\text{MF}} \sim kT$. Therefore, one can expect that the orientation of the chromophore molecule in liquid-crystalline medium will be dictated completely by the orientation potential of the matrix cage, i.e., by the orientation of adjacent molecules.

One more theoretical approach to photo-orientation is proposed by Palto and Durand.¹³ It explains the reorientation of the material by the collective torque exerted on the liquid crystal director by the subensemble of molecules in the excited state. According to this model, the motion of individual molecules can be described as rotation within the mean molecular field of the liquid-crystalline medium and short uncorrelated collisions between adjacent molecules. These collisions are assumed to induce sudden changes in frequencies and directions of molecular rotation. Considering the balance of torques for molecules in ground and excited states, the authors of this work¹³ come to a conclusion that the material director should change its orientation upon irradiation. The rate of director reorientation is defined by the expression

$$\tau_{\text{ph}}^{-1} = \frac{\tau_c}{J} \cdot I \ln 10 \varepsilon \tau_e W_{\text{MF}} \left| 1 - \frac{\eta}{\eta^*} \right| \Delta^2 \quad (14)$$

In eq 14, τ_{ph} is the characteristic time of director reorientation, τ_c is the average time between molecular collisions, J is the moment of inertia for the chromophore, I is the light intensity, expressed in $\text{Einstein}\cdot\text{s}^{-1}\cdot\text{cm}^{-2}$, ε is the extinction coefficient of the chromophore, τ_e is the average lifetime of molecules in the excited state, W_{MF} is the anisotropy of mean field potential, η and η^* are effective friction coefficients for chromophore molecules in the ground and excited state, and Δ is the half-width of orientation distribution function. The value of the effective friction coefficient is defined as $\eta = J \cdot W_{\text{MF}}^{-1} \cdot \tau_c^{-1}$.

The application of the discussed model to quantitative description of photo-orientation in azobenzene-containing liquid-crystalline polymer is complicated because of the unclear physical meaning of the parameter τ_c in glassy or liquid-crystalline matrix. Indeed, the model of reorientation through

free rotation interrupted by short random collisions seems to be oversimplified. In condensed matter, the molecules are constantly in contact with the surroundings, which limits the molecular rotation mobility. It is established that in liquid-crystalline,^{43,44} glassy,^{45,46} and polymer⁴⁷ media rotational motions of the molecules consist of angular vibrations restricted on amplitude by the matrix molecules. Reorientations by larger angles are cooperative motions, which include the rearrangement of the solvent cage around the molecule. The discussed model¹³ takes no account of the cooperative nature of molecular reorientation in condensed matter.

Realistic photo-orientation rates can be obtained within the discussed model if the average time between the collisions is assumed to be $\tau_c \sim 10^{-13} \text{ s}$.¹³ This value can be used to estimate rotation correlation time $\tau_R \sim \eta = J \cdot W_{\text{MF}}^{-1} \cdot \tau_c^{-1}$. Assuming $J \sim 10^{-42} \text{ kg}\cdot\text{m}^2$ and $W_{\text{MF}} \sim kT \sim 10^{-20} \text{ J}$, one obtains an estimate of $\tau_R \sim 10^{-9} \text{ s}$. This value is 7 orders of magnitude less than the lower estimate obtained in section B for the polymer PAAzo6 at 298 K. Thus, according to the discussed model,¹³ photo-orientation requires a much higher degree of rotation mobility than that experimentally observed in the liquid-crystalline polymer. As a result of these troubles, the discussed model does not demonstrate a predictive ability.

It should be noted that, according to the discussed model,¹³ photo-orientation of a monodomain sample should proceed through the rotation of the liquid-crystalline director with the invariance of the degree of orientation alignment. The measurements of orientation distribution in the course of photo-reorientation of PAAzo6 (see Figure 6b) do not support such behavior of orientation distribution function.

As far as we know, existing models do not account for the change in domain sizes during photo-orientation. Some models^{13,14} take into consideration the domain structure of photoaligning material. However, according to these models, photo-orientation proceeds inside the domain. Pedersen et al.¹⁴ have assumed that the interaction with adjacent domains impedes photo-orientation. Therefore, the model predicts that the larger the domain, the less is its surface per unit volume and the less should be the impeding effect of adjacent domains. Thus, according to this model, large domains should favor faster photo-orientation. This prediction contradicts the experimental observations. It is known that the enlargement of liquid-crystalline domains leads to slower and less effective photo-orientation.^{5,20,40}

An alternative model could be constructed using the idea that the large specific surface area of domain boundaries should facilitate the photo-orientation process. It was noted in ref 13 that reorientation of material in the vicinity of domain boundaries could be eased due to lower ordering and lower stability of the liquid-crystalline phase. Indeed, mesogenic molecules in the vicinity of domain boundaries can transit from one domain to another by means of a simple turn. This process requires neither large translational movement of the molecule nor alignment of photochromic molecules in defiance of the ordering potential of the cage. If for some reason the domains oriented along the electric field vector of light become less stable than the ones oriented in the perpendicular direction, then the process of domain structure rearrangement could lead to photo-orientation. The elaboration of this hypothesis constitutes the subject of the following paper.

E. CONCLUSIONS

A combination of optical methods and the spin probe technique was used in the present work for a detailed experimental study of photoinduced alignment of an azobenzene containing liquid-crystalline copolymer PAAzo6. The evolution of the material orientation distribution function was measured in the course of photo-orientation and photo-reorientation. The change in domain texture of the material during photo-orientation has been observed.

The analysis of existing models of photo-orientation has shown that they generally fail to account for experimentally observed features of photo-orientation in PAAzo6. In the oncoming paper, we shall formulate an alternative model based on photochemically induced rearrangement of the domain structure of liquid-crystalline material.

■ ASSOCIATED CONTENT

● Supporting Information

The detailed derivation of expressions 7 and 8 is given in Appendices A and B. This material is available free of charge via the Internet at <http://pubs.acs.org>.

■ AUTHOR INFORMATION

Corresponding Author

*E-mail: avbgdn@gmail.com.

Notes

The authors declare no competing financial interest.

■ ACKNOWLEDGMENTS

The authors are grateful to Dr. A. Yu. Bobrovsky and Dr. A. V. Ryabchun for provision of polymer PAAzo6 and to Prof. R. Tamura for provision of the spin probe. The financial support of Russian Foundation for Basic Research (Grant Nos. mol-a-12-03-31114, a-13-03-00648, ofi-m-13-03-12456, and mol-a-14-02-31882) is gratefully acknowledged. Some numerical calculations were performed with the use of Lomonosov Supercomputer at Moscow State University.

■ REFERENCES

- (1) Ikeda, T. Photomodulation of Liquid Crystal Orientations for Photonic Applications. *J. Mater. Chem.* **2003**, *13*, 2037–2057.
- (2) Yu, Y.; Ikeda, T. Alignment Modulation of Azobenzene-Containing Liquid Crystal Systems by Photochemical Reactions. *J. Photochem. Photobiol., C* **2004**, *5*, 247–265.
- (3) Cojocariu, C.; Rochon, P. Light-Induced Motions in Azobenzene-Containing Polymers. *Pure Appl. Chem.* **2004**, *76*, 1479–1497.
- (4) Hvilsted, S.; Sánchez, C.; Alcalá, R. The Volume Holographic Optical Storage Potential in Azobenzene Containing Polymers. *J. Mater. Chem.* **2009**, *19*, 6641–6648.
- (5) Bobrovsky, A.; Shibaev, V.; Hamplova, V.; Kaspar, M.; Glogarova, M. Chiroptical and Photooptical Properties of a Novel Side-Chain Azobenzene-Containing LC Polymer. *Monatsch. Chem.* **2009**, *140*, 789–799.
- (6) Zebger, I.; Rutloh, M.; Hoffman, U.; Stumpe, J.; Siesler, H. W.; Hvilsted, S. Photoorientation of a Liquid Crystalline Polyester with Azobenzene Side Groups. 1. Effects of Irradiation with Linearly Polarized Blue Light. *J. Phys. Chem. A* **2002**, *106*, 3454–3462.
- (7) Dumont, M.; Sekkat, Z. Dynamical Study of Photoinduced Anisotropy and Orientational Relaxation of Azo Dyes in Polymeric Films. Poling at Room Temperature. *Nonconducting Photopolymers and Applications, Proceedings of SPIE* **1992**, *1774*, 188–199.
- (8) Sekkat, Z.; Wood, J.; Knoll, W. Reorientation Mechanism of Azobenzenes within the Trans - Cis Photoisomerization. *J. Phys. Chem.* **1995**, *99*, 17226–17234.
- (9) Dumont, M. Dynamics of All-Optical Poling of Photoisomerizable Molecules. II: Comparison of Different Angular Redistribution Models. Theoretical and Experimental Study of Three-Dimensional Pumping. *J. Opt. Soc. Am. B* **2011**, *28*, 1855–1865.
- (10) Kiselev, A. Kinetics of Photoinduced Anisotropy in Azopolymers: Models and Mechanisms. *J. Phys.: Condens. Matter* **2002**, *14*, 13417–13428.
- (11) Chigrinov, V.; Pikin, S.; Verevochnikov, A.; Kozenkov, V.; Khazimullin, M.; Ho, J.; Huang, D.; Kwok, H.-S. Diffusion Model of Photoaligning in Azo-Dye Layers. *Phys. Rev. E* **2004**, *69*, 061713.
- (12) Kiselev, A.; Chigrinov, V.; Kwok, H.-S. Kinetics of Photoinduced Ordering in Azo-Dye Films: Two-State and Diffusion Models. *Phys. Rev. E* **2009**, *80*, 011706.
- (13) Palto, S. P.; Durand, G. Friction Model of Photo-induced Reorientation of Optical Axis in Photo-oriented Langmuir-Blodgett Films. *J. Phys. II* **1995**, *5*, 963–978.
- (14) Pedersen, T. G.; Johansen, P. M.; Holme, N. C. R.; Ramanujam, P. S. Theoretical Model of Photoinduced Anisotropy in Liquid-Crystalline Azobenzene Side-Chain Polyesters. *J. Opt. Soc. Am. B* **1998**, *15*, 1120–1129.
- (15) Kreuzer, M.; Benkler, E.; Paparo, D.; Casillo, G.; Marrucci, L. Molecular Reorientation by Photoinduced Modulation of Rotational Mobility. *Phys. Rev. E* **2003**, *68*, 011701.
- (16) Vorobiev, A. K.; Chumakova, N. A. Simulation of Rigid-Limit and Slow-Motion EPR Spectra for Extraction of Quantitative Dynamic and Orientational Information. In *Nitroxides - Theory, Experiment and Applications*; Kokorin, A. I., Ed.; InTech: Rijeka, Croatia, 2012; pp 57–112.
- (17) Vorobiev, A. K.; Yankova, T. S.; Chumakova, N. A. Orientation Distribution Function and Order Parameters of Oriented Spin Probe as Determined by EPR Spectroscopy. *Chem. Phys.* **2012**, *409*, 61–73.
- (18) Yankova, T. S.; Bobrovsky, A. Y.; Vorobiev, A. Order Parameters $\langle P_2 \rangle$, $\langle P_4 \rangle$, and $\langle P_6 \rangle$ of Aligned Nematic Liquid-Crystalline Polymer As Determined by Numerical Simulation of Electron Paramagnetic Resonance Spectra. *J. Phys. Chem. B* **2012**, *116*, 6010–6016.
- (19) Yankova, T. S.; Chumakova, N. A.; Pomogailo, D. A.; Vorobiev, A. K. Orientational Order of Guest Molecules in Aligned Liquid Crystal As Measured by EPR and UV-vis Techniques. *Liq. Cryst.* **2013**, *1*–11.
- (20) Bobrovsky, A.; Ryabchun, A.; Medvedev, A.; Shibaev, V. Ordering Phenomena and Photoorientation Processes in Photochromic Thin Films of LC Chiral Azobenzene-Containing Polymer Systems. *J. Photochem. Photobiol., A* **2009**, *206*, 46–52.
- (21) Ikuma, N.; Tamura, R.; Shimono, S.; Kawame, N.; Tamada, O.; Sakai, N.; Yamauchi, J.; Yamamoto, Y. Magnetic Properties of All-Organic Liquid Crystals Containing a Chiral Five-Membered Cyclic Nitroxide Unit Within the Rigid Core. *Angew. Chem., Int. Ed. Engl.* **2004**, *43*, 3677–3682.
- (22) Chumakova, N. A.; Vorobiev, A. K.; Ikuma, N.; Uchida, Y.; Tamura, R. Magnetic Characteristics and Orientation of a New Nitroxide Radical in an Ordered Matrix. *Mendeleev Commun.* **2008**, *18*, 21–23.
- (23) Mauser, H.; Gauglitz, G. *Photokinetics, Theoretical Fundamentals and Applications*; Elsevier: Amsterdam, The Netherlands, 1998; Vol. 36.
- (24) Martinez-Ponce, G.; Petrova, T.; Tomova, N.; Dragostinova, V.; Todorov, T.; Nikolova, L. Investigations on Photoinduced Processes in a Series of Azobenzene-Containing Side-Chain Polymers. *J. Opt. A: Pure Appl. Opt.* **2004**, *6*, 324–329.
- (25) Chernova, D. A.; Vorobiev, A. K. H. Molecular Mobility of Nitroxide Spin Probes in Glassy Polymers. Quasi-Libration Model. *J. Polym. Sci., Part B: Polym. Phys.* **2009**, *47*, 107–120.
- (26) Osipov, M. A.; Terentjev, E. M. Statistical Viscosity Theory of Nematic Liquid Crystals. *Phys. Lett. A* **1989**, *134*, 301–306.
- (27) Buka, A.; de Jeu, W. H. Diamagnetism and Orientational Order of Nematic Liquid Crystals. *J. Phys. (Paris)* **1982**, *43*, 361–367.
- (28) Budil, D. E.; Lee, S.; Saxena, S.; Freed, J. H. Nonlinear-Least-Squares Analysis of Slow-Motion EPR Spectra in One and Two

Dimensions Using a Modified Levenberg–Marquardt Algorithm. *J. Magn. Reson., Ser. A* **1996**, *120*, 155–189.

(29) Carr, S. G.; Khoo, S. K.; Luckhurst, G. R.; Zannoni, C. On the Ordering Matrix for the Spin Probe (3-spiro [2'-N-oxyl-3',3'-dimethyloxazolidine])-5 α -cholestane, in the Nematic Mesophase of 4,4'-dimethoxyazoxybenzene. *Mol. Cryst. Liq. Cryst.* **1976**, *35*, 7–13.

(30) Gurp, M. v. The Use of Rotation Matrices in the Mathematical Description of Molecular Orientations in Polymers. *Colloid Polym. Sci.* **1995**, *273*, 607–625.

(31) Zannoni, C. Distribution Functions and Order Parameters. In *The Molecular Physics of Liquid Crystals*; Luckhurst, G. R., Gray, G. W., Eds.; Academic Press: London, 1979; pp 51–83.

(32) Rau, H. Azo Compounds. In *Photochromism. Molecules and systems*; Durr, H., Bouas-Laurent, H., Eds.; Elsevier: Amsterdam, The Netherlands, 2003; pp 165–192.

(33) Statman, D.; Jánossy, I. Study of Photoisomerization of Azo Dyes in Liquid Crystals. *J. Chem. Phys.* **2003**, *118*, 3222–3232.

(34) Loucif-Saïbi, R.; Nakatani, K.; Delaire, J. A.; Dumont, M.; Sekkat, Z. Photoisomerization and Second Harmonic Generation in Disperse Red One-Doped and -Functionalized Poly(methyl methacrylate) Films. *Chem. Mater.* **1993**, *5*, 229–236.

(35) Sekkat, Z.; Yasumatsu, D.; Kawata, S. Pure Photoorientation of Azo Dye in Polyurethanes and Quantification of Orientation of Spectrally Overlapping Isomers. *J. Phys. Chem. B* **2002**, *2002*, 12407–12417.

(36) Cusati, T.; Granucci, G.; Martinez-Nunez, E.; Martini, F.; Persico, M.; Vazquez, S. Semiempirical Hamiltonian for Simulation of Azobenzene Photochemistry. *J. Phys. Chem. A* **2012**, *116*, 98–110.

(37) Pedersen, T. G.; Ramanujam, P. S.; Johansen, P. M. Quantum Theory and Experimental Studies of Absorption Spectra and Photoisomerization of Azobenzene Polymers. *J. Opt. Soc. Am. B* **1998**, *15*, 2721–2730.

(38) Yankova, T. S.; Chumakova, N. A.; Pomogailo, D. A.; Vorobiev, A. K. Spin Probe Orientation Distribution Functions in Aligned Nematic Liquid Crystal. *Magn. Reson. Solids* **2011**, *13*, 10–13.

(39) *Smart Light-Responsive Materials. Azobenzene-Containing Polymers and Liquid Crystals*; John Wiley & Sons: Hoboken, NJ, 2009.

(40) Zakrevskyy, Y.; Stumpe, J.; Smarsly, B.; Faul, C. Photoinduction of Optical Anisotropy in an Azobenzene-Containing Ionic Aelf-Assembly Liquid-Crystalline Material. *Phys. Rev. E* **2007**, *75*, 031703.

(41) Grebenkin, S. Y.; Bol'shakov, B. V. Photo-Orientation of Azo Dye Molecules in Glassy o-terphenyl. *J. Photochem. Photobiol., A* **2006**, *184*, 155–162.

(42) Albrecht, A. C. Photo-Orientation. *J. Chem. Phys.* **1957**, *27*, 1413–1414.

(43) Janik, J. A.; Godlewska, M.; Grochulski, T.; Kocot, A.; Sciesinska, E.; Sciesiski, J.; Witko, W. Molecular Reorientation in Liquid Crystals. *Mol. Cryst. Liq. Cryst.* **1983**, *98*, 67–81.

(44) Lalanne, J.; Destrade, C.; Nguyen, H.; Marcerou, J. Fast Molecular Reorientations in Liquid Crystals. *Phys. Rev. A* **1991**, *44*, 6632–6640.

(45) Hunt, B. I.; Powles, J. G. Nuclear Spin Relaxation and a Model for Molecular Reorientation in Supercooled Liquids and Glasses. *Proc. Phys. Soc.* **1966**, *88*, 513–528.

(46) Polimeno, A.; Freed, J. H. Slow motional ESR in complex fluids: the slowly relaxing local structure model of solvent cage effects. *J. Phys. Chem.* **1995**, *99*, 10995–11006.

(47) Chernova, D. A.; Vorobiev, A. K. Molecular Mobility of Nitroxide Spin Probes in Glassy Polymers: Models of the Complex Motion of Spin Probes. *J. Appl. Polym. Sci.* **2011**, *121*, 102–110.